Proceedings of the 58th Canadian Geotechnical Conference, Saskatoon, Canada.Vol.2. pp. 410-415. September, 18-21. 2005

ROLE OF MATRIC SUCTION IN THE INTERPRETATION OF UNCONFINED COMPRESSION TESTS

KATO, Shoji, Kobe University, Japan
YOSHIMURA, Yuji, Gifu National Institute of Technology, Japan
FREDLUND, Delwyn G., University of Saskatchewan, Saskatoon, Sask., Canada, STJ3B9

ABSTRACT
This paper reports the results of a study in which matric suction and volume change of soil specimens were measured on specimens tested in unconfined compression. The tests were conducted on both statically and dynamically compacted specimens of silty clay. The effective shear strength parameters; namely, c', effective cohesion, and ϕ', angle of internal friction, were measured on saturated soil specimens. The results of the unconfined compression tests were interpreted within the context of the extended Mohr-Coulomb shear strength theory by giving consideration to the fundamental components of shear strength. The test result allowed a cohesion component of shear strength that is associated with the effect of dry density to be separated from the other components of shear strength.

RÉSUMÉ
Cet article presente une etude dans laquelle la succion matricielle et le changement de volume d'echantillon du sol ont ete mesures sur des echantillons en compression non confiee. Les essais ont ete realises statiquement et dynamiquement sur les specimens de l'argilite silty. Les parametres de la resistance au cisaillement, nomme la cohesion effective et l'angle de frottement interne, ont ete obtenus par des eprouvettes de sol sature. Ensuit, les resultats des essais de compression non confinee ont ete interpretes dans la contexte de la theorie de la resistance au cisaillement des sols en prenant en compte des composants fondamentaux de resistance au cisaillement. Les resultats des essais ont permis que un composant de cohesion de la resistance au cisaillement, qui est relie avec l'effet de densite seche, soit separe de l'autre composant.

1. INTRODUCTION

The unconfined compression test is widely used inside Japan for the design of geotechnical-engineered structures. Soil specimens used for the unconfined compression test are often in an unsaturated state, and negative pore-water pressures equal to the matric suction. Since no confining pressure is applied to soil specimen in the unconfined compression test, it is primarily the matric suction that controls the measured shear strength. There are few studies that attempt to interpret the unconfined compressive strength obtained through the matric suction and its effects.

In the past study of the unconfined compression test, research has been undertaken on unsaturated soils near high degrees of saturation. Mitachi & Kudoh (1996) and Shimizu & Tabuchi (1993) showed experimental test results and used the Terzaghi's effective stress concept to explain the unconfined compressive strength of nearly saturated soils. In these studies, the matric suction has a role of applying a confining pressure under a high degree of saturation.

Ridley (1995) took the unconfined compression test as one of undrained test, and showed a unique relationship between the "critical water content" and the suction. In this study, the unconfined compression tests, in which the suction was measured, were carried out for statically and dynamically compacted silty clay specimens. The relationships of the matric suction with the unconfined compressive strength, and the relationship between the matric suction and cohesion are examined. The results of the unconfined compression tests were interpreted within the context of the extended Mohr-Coulomb shear strength theory by giving consideration to the fundamental components of shear strength.

2. SHEAR STRENGTH PARAMETERS AND UNCONFINED SOMPRESSIVE STRENGTH OF UNSATURATED SOIL

2.1 Shear Strength of Unsaturated Soil

Soil-water exits as menisci at the contact points between particles of an unsaturated soil. A pressure difference is induced between pore-air pressure and pore-water pressure that is called as the matric suction. Suction causes intergranular adhesive forces between particles perpendicular to the contact plane. The influence of the matric suction results in a complex behavior of the unsaturated soil.

Fredlund et al. (1978) proposed an equation to represent shear strength for unsaturated soil.

$$[1]\ \tau = c_{sat} + (\sigma - u_a)\tan\phi_{sat} + (u_a - u_w)\tan\phi^b$$

where: τ = shear stress at failure on the failure plane; σ = normal total stress at failure on the failure plane; c_{sat} = cohesion under saturated conditions; ϕ_{sat} = internal friction angle under the saturated state; ϕ^b = parameter related to

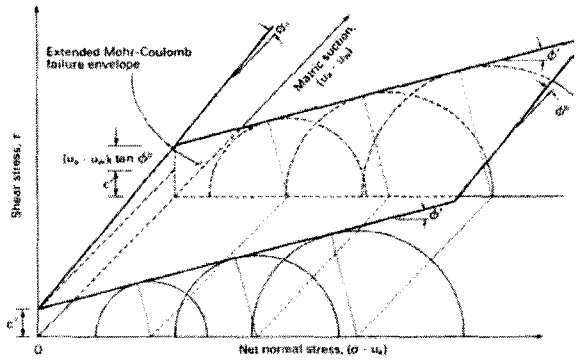

Figure 1: Extended Mohr-Coulomb failure envelope for unsaturated soils (Fredlund & Rahardjo, 1993)

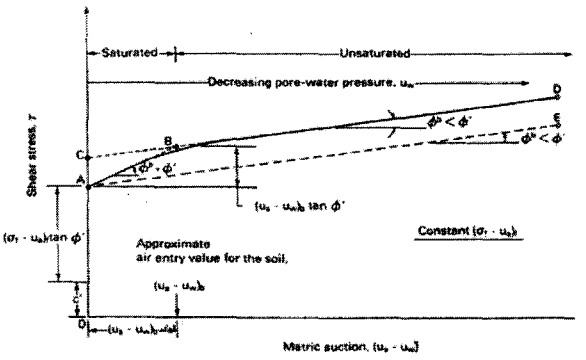

Figure 2: Non-linearity of the failure envelope on the τ versus $(u_a - u_w)$ plane (Fredlund & Rahardjo, 1993)

the increase of shear strength with suction increase and u_a, u_w = pore-air and pore-water pressure, respectively.

The relationship between the shear strength, τ, and the two stress state variables, $(\sigma - u_a)$ and $(u_a - u_w)$, can be represented using a three-dimensional plot as shown in Figure 1. In this figure, the frontal plane represents a saturated soil where the matric suction is zero, and Mohr circles for an unsaturated soil are plotted with respect to the net normal stress axis in the same manner as the Mohr circles are plotted for saturated soils with respect to effective stress.

The surface tangent to the Mohr circles at failure is referred to as the extended Mohr-Coulomb failure envelope for an unsaturated soil. It is a curved failure envelope that intersects the shear stress axis giving a cohesion intercept, c', and has slope angles of ϕ' and a variable ϕ^b with respect to net normal stress and matric suction, respectively.

Shear strength test results on unsaturated soils indicate non-linearity in the shear strength versus matric suction failure envelope (Escario and Saez, 1986). Figure 2 illustrates a typical non-linear matric suction failure

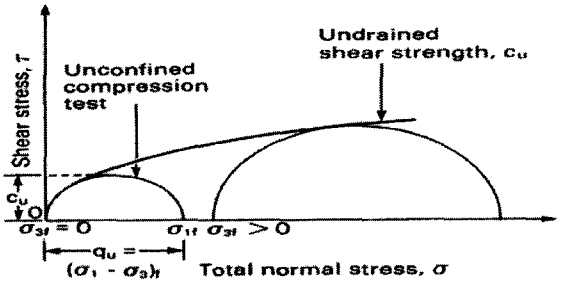

Figure 3: Relationship between q_u and c_u for a unsaturated soil (Fredlund & Rahardjo, 1993)

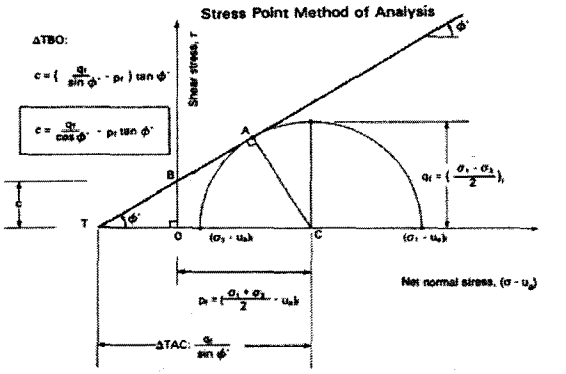

Figure 4: Analytical procedure to obtain the cohesion intercept from a single Mohr circle (Fredlund & Rahardjo, 1993)

envelope. The ϕ^b angle appears to be equal to ϕ' at low matric suctions and decreases to a lower value at high matric suctions. This means that the angle ϕ^b is a function of the matric suction.

2.2 Relationship between Undrained Strength and Unconfined Compressive Strength of Unsaturated Soil

Unconfined compression test results on the unsaturated soil apply to the condition where the total confining pressure is equal to zero (Figure 3). In the unconfined compression test, the deviator stress at failure is referred to as the unconfined compressive strength, q_u. The unconfined compressive strength is commonly taken as being equals to twice the undrained shear strength, c_u at a confining pressure greater than zero. As the confining pressure increases, the undrained shear strength for the unsaturated soil also increases. As a result, the compressive strength value may not provide a satisfactory means of approximating the undrained shear strength, c_u.

Figure 4 shows an analytical procedure that can be used to obtain the cohesion intercept from a single Mohr circle. A Mohr circle at failure is constructed with its

corresponding p_f and q_f values. A failure envelope with a slope angle of ϕ' is drawn tangent to the Mohr circle at point *A*. The envelope intersects the shear strength axis at point *B* and the $(\sigma - u_a)$ axis at point *T*. The cohesion intercept, *c*, is computed from triangle *TBO*, as illustrated in Figure 4. The cohesion intercepts, *c*, at various matric suctions can be computed from the above equation and plotted on the shear strength versus the matric suction plane to obtain the angle, ϕ^b. In the case of the unconfined compression test, $(\sigma_3 - u_a)$ is equal to zero, and if we know the value of ϕ', the cohesion intersect can be calculated using the same procedure mentioned above.

3. TEST PROCEDURE

3.1 Soil Sample Used for the Tests

A non-plastic silty clay, whose specific gravity of the soil particles, G_s is 2.68, was used. After adding distilled water to the air-dried sample in order to adjust water content, it was stored for one day in a sealed container.

3.2 Preparation of Statically Compacted Specimen

The wetted sample was statically compacted in a mold with dimensions of 50mm diameter and 300mm height. The inside of this mould was coated with Teflon. When the wetted sample was compacted in the mold, a spacer disk was used in order to adjust the specimen height to 120mm. The dry densities were set for three values of 1.250, 1.330 and 1.405 g/cm^3. The water contents were adjusted to 3%-24% for the preparation of the specimens. After coating the sample with a plastic film and wrapping it with a wetted cloth to prevent the drying of the compacted specimen, it was stored for a few days in a closed container, and taken out before the test. By removing a portion of the top and bottom of the compacted sample, a specimen of 50mm diameter and 100mm height was made.

3.3 Preparation of Dynamically Compacted Specimen

Dynamically compacted specimens were made in a mold of 10 cm diameter using rammer of 2.5 kg. A compacted sample was made using five layers and each layer was compacted with 25 and 50 times of tamping. Figure 5 shows the compaction curve for specimens prepared using 25 tampings. The water contents in the unconfined compression tests were 11 to 23%. The optimum water content was about 18%. The compacted samples were kept in a closed container and trimmed before each test to a specimen size of 50 mm diameter and 100 mm height. These prepared specimens were used in the unconfined compression tests.

3.4 Unconfined Compression Test Measuring Suction and Volume Change of Each Specimen

Figure 6 shows a sketch of the unconfined compression test cell. After the specimen was set on the pedestal of

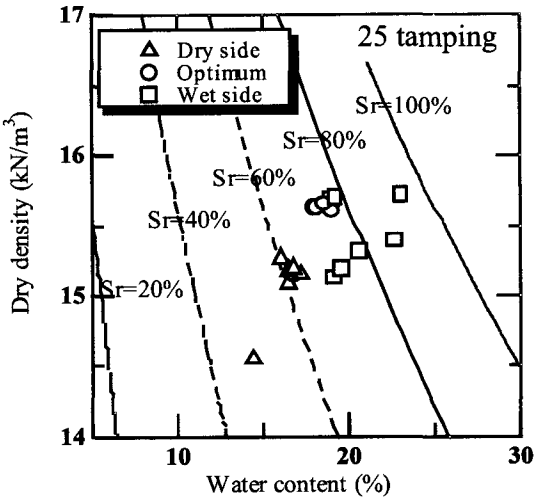

Figure 5: Compaction curve data for silty clay

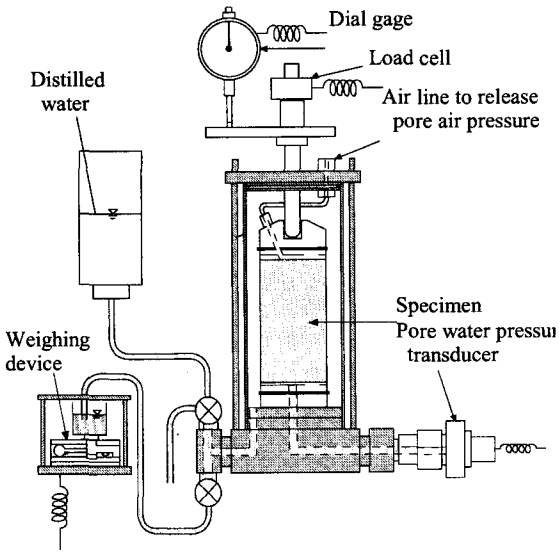

Figure 6: Sketch of unconfined compression test cell apparatus

the cell, the specimen was covered with a rubber membrane and a loading cap, and sealed with O-rings. Before the test was carried out, the cell was filled with water. During the test, the displacement of the cell water was measured with a weighing device that was connected to the inside of the cell. The volume of the specimen was obtained from adjusting the recorded displacement of the cell water for the piston penetration into the cell. A ceramic disk, whose air entry value was 500 kPa, was sealed into the pedestal of the cell to measure the pore-water pressure in the specimen. In the loading cap, a porous metal plate was installed. An air line was connected to the loading cap and the pore-air pressure in the specimen was released to atmosphere. The suction in

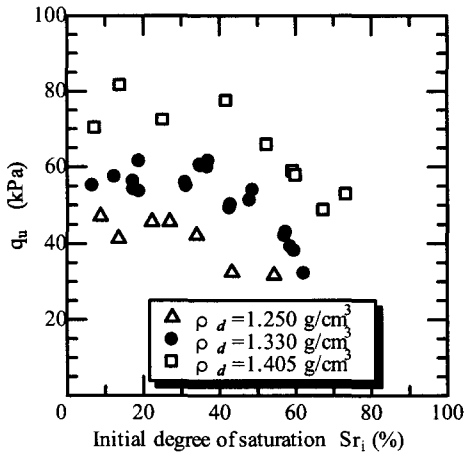

Figure 7: Relationship between unconfined compressive strength and the initial degree of saturation for statically compacted specimens

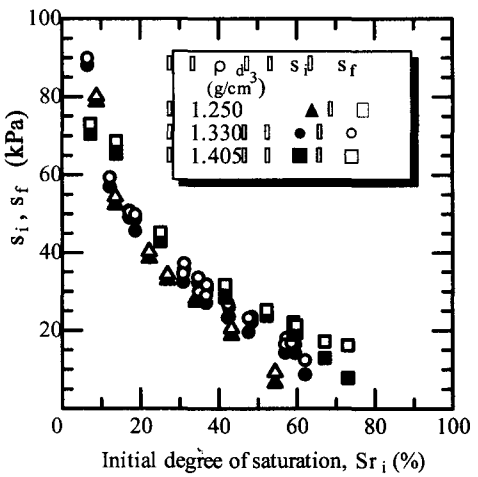

Figure 8: Relationship between initial suction, suction at failure and initial degree of saturation for statically compacted specimens

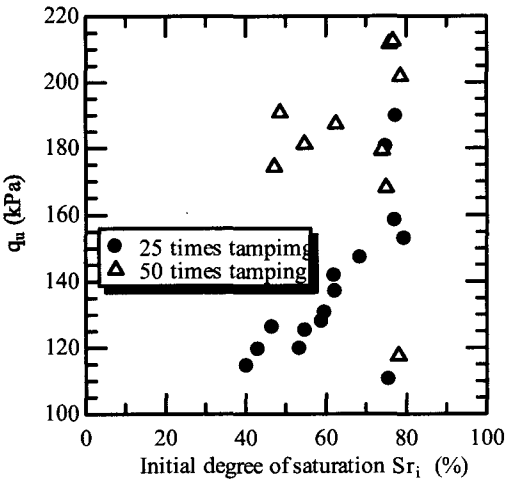

Figure 9: Relationship between unconfined compressive strength and the initial degree of saturation for dynamically compacted specimens

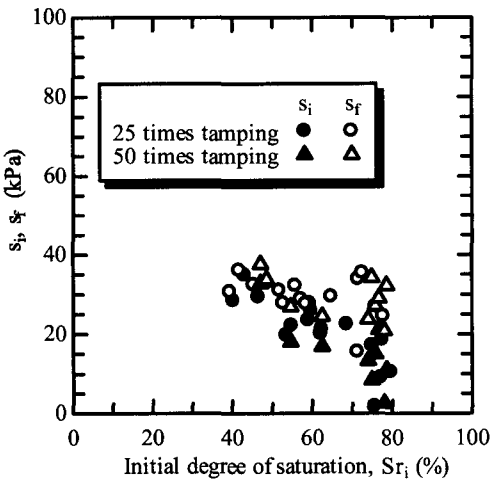

Figure 10: Relationship between initial suction, suction at failure and initial degree of saturation for dynamically compacted specimens

the specimen was decided from the value of the measured pore-water pressure. The rate of strain used was 0.1% per minute.

4. TEST RESULTS AND DISCUSSION

4.1 Unconfined Compressive Strength

Figure 7 shows the relationship between the unconfined compressive strength, q_u and the initial degree of saturation, S_{ri}, which was measured when the specimen was trimmed for statically compacted specimen. The unconfined compressive strength increases when the dry density increases. Up to 40 to 50% degrees of saturation, the unconfined compressive strengths remain almost constant in each case, respectively. But the unconfined compressive strength decreases when the degree of saturation is further increased. It was found that the optimum water content is not clear from these results.

Figure 8 shows the relationship between the initial suction, s_i, the suction at failure and s_f with the initial degree of saturation, S_{ri}. The s_i and s_f values decrease with an increase in S_{ri} for statically compacted specimens. But the amounts of increase in suction, $\Delta(s_f-s_i)$, gradually become

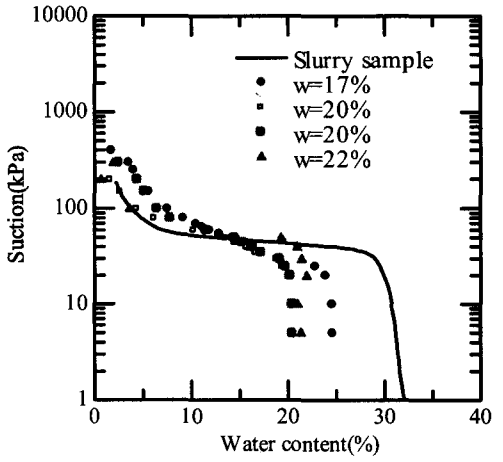

Figure 11: Soil-water characteristic curve for the soil

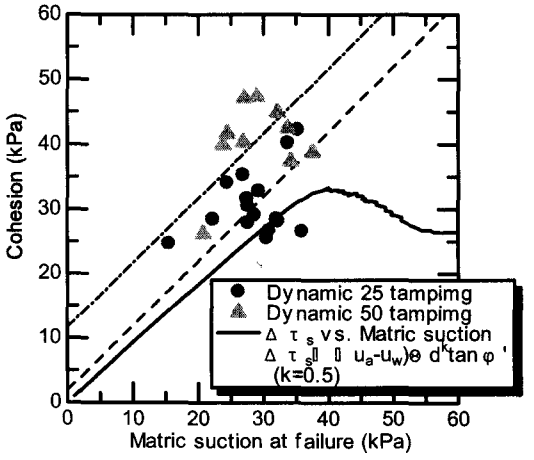

Figure 12: Relationship between cohesion and matric suction for dynamically compacted specimens

larger when S_{ri} increases, and any effect of the density is hardly observed. The reason why matric suction increases during the shear process for the statically compacted specimen, is not clear

Figure 9 shows the variation in unconfined compressive strengths with the initial degree of saturations for dynamically compacted specimen. The unconfined compressive strength increases as the initial degree of saturation increases to 80% which is near to the optimum water content. It then drops rapidly when the degree of saturation further increased. This tendency is different from that observed in Figure 7 for statically compacted specimens.

Figure10 shows the variation in the initial suction and the suction at failure with the initial degree of saturation for dynamically compacted specimen. The initial suction

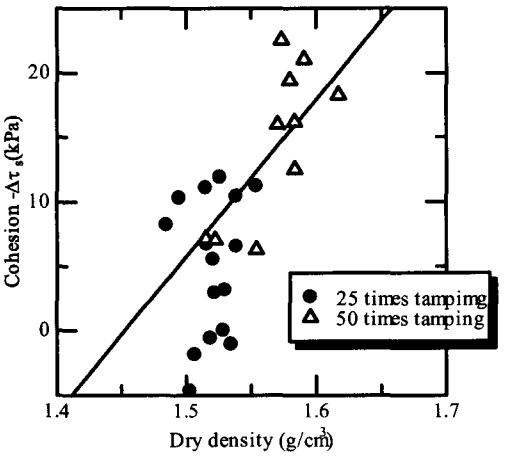

Figure 13: Difference in cohesion vs. dry density for dynamically compacted specimens

decreases as the initial degree of saturation increases, but the suction at failure gradually decreases, and then increases. The suction in all of the specimens increases from the initial state to failure. It was found that the increase in suction become larger when the specimen has a high initial degree of saturation. This behaviour seems to correspond to that observed in Figure 9, but it is clearer because of the effect of dry density.

From Figures 9 and 10, it is understood that even if the suction decreases with an increase in the degree of saturation, the unconfined compressive strength does not show the same tendency. This result means that not only the suction but also the soil structure has influence on the unconfined compressive strength.

4.2 Cohesion Components of Shear Strength

In Figure 11, the solid curve shows the soil-water characteristic curve (SWCC) for the silty clay in a slurry condition, and the dots show the SWCC for dynamically compacted specimens under different initial water contents. The SWCC for the slurry condition is different from that for the compacted specimens, and these results show that each specimen has a different soil structure.

The increased shear strength component attributable to suction, $\Delta\tau_s$, is predicted by the next equation with the SWCC. (Fredlund et al. 1996)

$$[2]\ \Delta\tau_S = (u_a - u_w)\,\Theta^{\kappa}\tan\phi'$$

where: Θ = normalized water content as a function of matric suction, and
κ = soil parameter depending upon the soil type.

In Figure 12, the solid curve shows the change in strength, $\Delta\tau_S$, versus matric suction obtained by using Equation (2) for the SWCC for slurry specimens in Figure

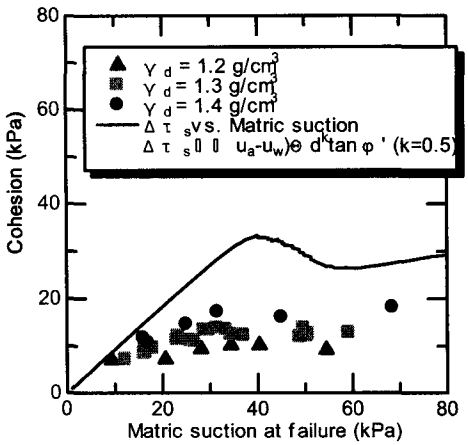

Figure 14: Relationship between cohesion and matric suction for statically compacted specimens

11. The dots show the relationship between cohesion and matric suction at failure for dynamically compacted specimens. Here, the cohesions are calculated using the procedure shown in Figure 4. The dashed line and the dotted line are the regression lines for the dynamically compacted specimens with different tamping times. Almost all the dots exist above the curve. This means that the cohesion in the dynamically compacted specimens is larger than the cohesion induced by suction when starting from a slurry state. The soil structure must affect on the shear strength of the unsaturated soil.

Figure 13 shows the relation between the calculated differences in shear strength (cohesion - $\Delta\tau_s$), versus the dry density of the dynamically compacted specimens. The solid line is the regression line for the positive values of (cohesion - $\Delta\tau_s$) for the dynamically compacted specimens. From this figure, it can be seen that the dry density has an influence on the increase in the shear strength component for the dynamically compacted specimens.

Figure 14 shows a similar relationship to Figure 12 for the statically compacted specimens. In this figure, the solid curve is the $\Delta\tau_s$ versus matric suction relationship. The relationship between cohesion and matric suction shows a differing behavior for different dry densities. The cohesion in the statically compacted soil specimens is lower than the $\Delta\tau_s$ versus matric suction relationship. This shows a different tendency than that observed in Figure 12. This result also shows that the statically compacted specimen have a different soil structure from that of the slurry soil, and the soil structure influences the shear strength for the statically compacted specimens.

5. CONCLUDING REMARKS

Matric suction and volume change of soil specimens were measured on specimens tested in unconfined compression, and the results of the unconfined compression tests were interpreted within the context of the extended Mohr-Coulomb shear strength theory by giving consideration to the fundamental components of shear strength. The components of shear strength used for the interpretation of the statically compacted specimens consisted of: i.) an effective cohesion component, ii.) a frictional component (since the failure envelope is tangent to the Mohr circles), and iii.) a matric suction component. The matric suction component was determined by measuring the matric suction and also using the soil-water characteristic curve, SWCC, measured on the silty clay soil. The unconfined compression strengths on the statically compacted soil specimens prepared at a particular density agree quite closely to the extended Mohr-Coulomb shear strength equation shown in Equation (1).

The unconfined compressive strengths of the dynamically compacted specimens showed an increase in strength, in terms of a cohesion component, that was related to the dry density of the soil. The test results allowed the cohesion component of shear strength that is associated with the effect of dry density to be separated from other components of shear strength.

References

Escario, V. and Saez, J. 1986, Shear strength of partly saturated soils, *Geotechnique*, 36(3): pp. 453-456.

Fredlund, D.G., Morgenstern, N.R. and Widger, R.A. 1978, The shear strength of unsaturated, *Can. Geotechnical Journal*, 15: pp. 313- 321.

Fredlund, D. G. and Rahardjo, H. 1993, *Soil mechanics for unsaturated soils*, John Wiley & Sons.

Fredlund, D.G., Xing, A., Fredlund, M.D. and Barbour, S.L. 1996, The relationship of the unsaturated soil shear strength to the soil-water characteristic curve, *Can. Geotechnical Journal*, 33: pp. 440-448.

Mitachi, T. and Kudo, Y. 1989, Method for predicting in-situ undrained strength of clays based on the suction value and unconfined compressive strength *Journal of Japanese Society of Civil Engineering*, 541: pp. 147-158.

Ridley A. M. 1995, Strength-Suction-Moisture Content Relationships for Kaolin under Normal Atmospheric Conditions, *Unsaturated Soils*, Balkema, 1: pp. 645-651.

Shimizu, S. and Tabuchi, T. 1993, Effective Stress Behavior of Clays in Unconfined Compression Tests, *Soils and Foundations*, 33(3): pp. 28-39.